Anisotropic intrinsic anomalous Hall effect in epitaxial Fe films on GaAs(111)

Lin Wu, Yufan Li, Jianli Xu, Dazhi Hou, and Xiaofeng Jin*

Department of Physics, State Key Laboratory of Surface Physics, Fudan University, Shanghai 200433,China

(Received 5 February 2013; published 15 April 2013)

The anomalous Hall effect (AHE) in epitaxial Fe films on GaAs(111) has been investigated as a function of film thickness and temperature. The intrinsic contribution from the Berry curvature is singled out from the extrinsic ones and determined to be 821 Ω^{-1} cm^{-1}, which agrees to the theoretical prediction of 842 Ω^{-1} cm^{-1} and is considerably smaller than 1100 Ω^{-1} cm^{-1} for Fe(001). This result provides a direct experimental evidence for the anisotropy of the intrinsic AHE in single crystal Fe, reflecting its electronic band structure.

DOI: 10.1103/PhysRevB.87.155307 PACS number(s): 75.47.Np, 71.70.Ej, 72.15.Eb, 73.50.Jt

The anomalous Hall effect (AHE) is a fascinating phenomenon in condensed matter physics. In its century-long history, three mechanisms have been identified: the intrinsic contribution[1,2] and the extrinsic contributions, which include the skew scattering,[3,4] and the side jump.[5] The two extrinsic mechanisms are related to the asymmetric scattering for spin-up and spin-down electrons, while the intrinsic mechanism is material specific and dictated by the electronic band structure. Furthermore, the intrinsic mechanism can be reformulated as a Berry curvature contribution, which enables the first-principles calculation of the intrinsic anomalous Hall conductivity (AHC).[6–10] Due to the anisotropy of the Berry curvature in the momentum space, the intrinsic AHE is expected to show the anisotropic behaviors.[11–13]

Theoretically, the anisotropy of the intrinsic AHE has been investigated in 3*d* transition metals and their alloys.[12–14] In hcp Co, the intrinsic AHC for **M** along the *c* axis (the magnetic easy axis) and *a* or *b* axis (the hard axis) are predicted to be about 480 and 100 Ω^{-1} cm^{-1}, respectively.[12,13,15] In bcc Fe, the calculations for [100] (the easy axis) and [111] (the hard axis) crystalline axes give the values of 767 and 842 Ω^{-1} cm^{-1}, respectively.[13,16] However, considering the fact that both the intrinsic AHE and the magnetocrystalline anisotropy share the same origin from the intrinsic spin-orbit coupling, these results are intuitively inconsistent with those of the magnetocrystalline anisotropy, for the intrinsic AHC for the easy axis in Co is larger than that for the hard axis while it is just the opposite in Fe. Therefore, it is interesting to explore in experiment the connection between the AHE and the magnetocrystalline anisotropy.

Experimentally the anisotropic behavior of the AHE was indeed realized in several magnetic materials.[17–23] But they are all the total rather than the intrinsic AHE. So far it has never been clarified whether the anisotropy originates from the intrinsic mechanism or the extrinsic mechanism. Recently the intrinsic AHC of bcc Fe(001) has been experimentally disentangled with the extrinsic contributions and determined to be 1100 Ω^{-1} cm^{-1},[24] which is consistent with the results from Fe whisker.[25] Naturally bcc Fe(111) now becomes an intriguing system to study the anisotropy of the intrinsic AHE, which might help to establish the connection between the transport and magnetic properties of Fe. In this paper we report the transport measurement of the AHE in Fe(111) films epitaxially grown on GaAs(111) by tuning the film thickness as well as temperature, and determine the intrinsic AHC to be 821 ± 13 Ω^{-1} cm^{-1} which support the theoretical prediction 842 Ω^{-1} cm^{-1}[13] but much smaller than 1100 Ω^{-1} cm^{-1} in Fe(001).[24] It is an unambiguous experimental evidence for the anisotropy of the intrinsic AHE.

Fe thin films with film thickness ranging from 4 to 27 nm were epitaxially grown with several steps on undoped GaAs(111) at room temperature, as shown in Fig. 1(a). Prior to growth, in order to remove surface oxidation and other contaminants, GaAs(111) substrates were cleaned by argon ion bombardment for 2 h, followed by annealing at 560 °C with the presence of argon ion bombardment for half an hour, so that the reflection high-energy electron diffraction (RHEED) pattern of 2×2 reconstruction is clearly seen,[26] as shown in Fig. 1(b). The Fe films grew in bcc structure, as verified by the RHEED patterns [Fig. 1(c)].[27] Finally, about 4 nm MgO was evaporated on top as a protection layer. Standard Hall bar of the size 200 μm $\times$ 500 μm was patterned on each thickness step by photolithograph and wet etching. The transport measurements of thin films Fe(111) were taken in the physical properties measurement system (PPMS).

Figure 2(a) shows the temperature dependence of longitudinal resistivity ρ_{xx} for several film thicknesses d ranging from 4 to 27 nm with the current along GaAs[11$\bar{2}$]. Above 4 nm the full development of Berry curvature is guaranteed.[24] According to Matthiessen law, at the finite temperature, ρ_{xx} can be decomposed into the residual resistivity ρ_{xx0} induced by impurity scattering, and ρ_{xxT} originating from the elementary excitation, such as phonon and magnon, i.e., $\rho_{xx} = \rho_{xx0} + \rho_{xxT}$. Figure 2(b) shows the decay of ρ_{xx0} as a function of film thickness, which shows strong finite size effect.[28,29] Now the resistivity can be tuned in two ways by varying either the temperature at a fixed film thickness or vice versa. Several representative sets of ρ_{xy} vs B curves for 27 nm Fe film are displayed in Fig. 2(c). The anomalous Hall resistivity $\rho_{ah}(T)$ is then obtained as the zero-field extrapolation of the high field data as shown in the figure. The temperature and thickness dependence of anomalous Hall resistivity are summarized in Fig. 2(d).

Following the procedure to disentangle the intrinsic and extrinsic AHE contributions by the scaling:[24,30,31]

$$-\sigma_{ah} = \left(\alpha\sigma_{xx0}^{-1} + \beta\sigma_{xx0}^{-2}\right)\sigma_{xx}^{2} + b, \qquad (1)$$

where σ_{ah} is the AHC, σ_{xx} and σ_{xx0} denote the longitudinal conductivity at finite temperature, and $T \rightarrow 0$ K, respectively, α is the parameter of the skew scattering, β denotes the side jump, and b is the intrinsic AHE. We plot σ_{ah} as a function

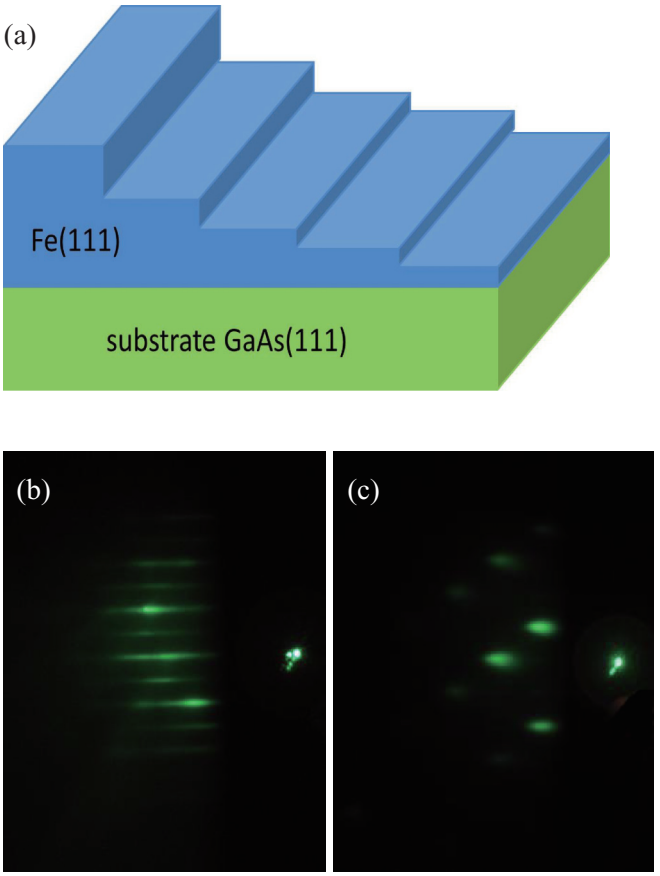

FIG. 1. (Color online) (a) The schematic of the as-grown bcc Fe(111) thickness steps sample. (b) The RHEED pattern of GaAs(111) substrate taken along [1$\bar{1}$0]. (c) The RHEED pattern of Fe(111) film taken along GaAs[1$\bar{1}$0].

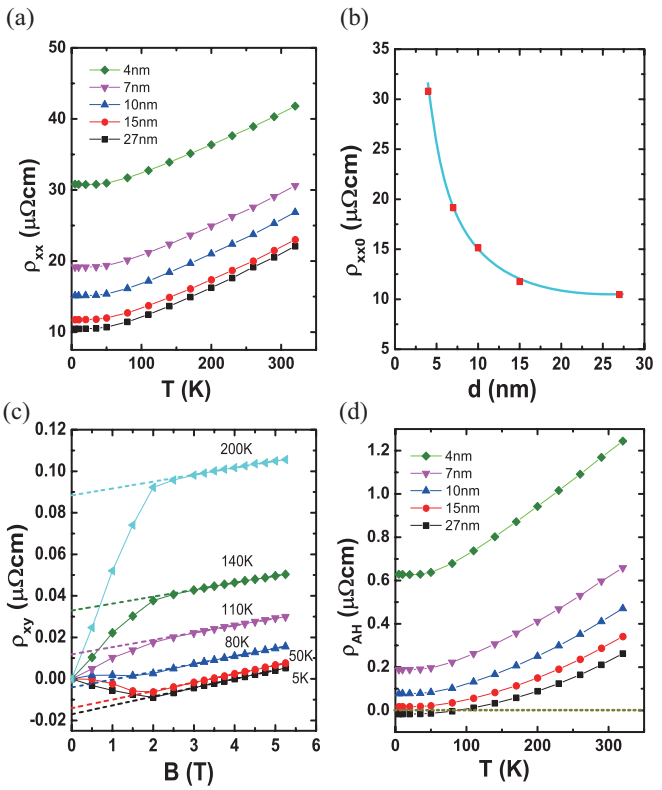

FIG. 2. (Color online) (a) The temperature dependence of the longitudinal resistivity for various Fe film thicknesses. (b) The thickness dependence of residual resistivity ρ_{xx0}. Here the resistivity measured at 5 K is taken as ρ_{xx0}. The blue line is a guide for the eyes. (c) The Hall resistivity of 27 nm Fe for various temperatures. The dashed lines are the extrapolation from the high field to zero field for deriving the anomalous Hall resistivity. (d) The plot of the anomalous Hall resistivity versus temperature. All transport measurements are conducted by applying the current along GaAs[11$\bar{2}$] direction.

of σ_{xx}^2 in Fig. 3(a). Similar to the Fe(100) case, a converged intercept is clearly observed. The thickness-independent b is reassuring that the averaged value $821 \pm 17\ \Omega^{-1}\ \mathrm{cm}^{-1}$ is the intrinsic AHC of Fe(111) that comes from the Berry curvature contribution determined by the band structure. The AHE in principle depends on the direction of current with respect to the crystalline axis, so we also carried out the measurement by applying the current along GaAs[1$\bar{1}$0] direction, while the magnetic field remains along the Fe[111] direction. The result is plotted in Fig. 3(b), in which a converged intercept is realized again [see also the inset of Fig. 3(a) for the summarized intercepts]. The intrinsic AHC for $I \parallel$GaAs[1$\bar{1}$0] is therefore determined to be $859 \pm 20\ \Omega^{-1}\ \mathrm{cm}^{-1}$. The agreement of these two cases, one with $I \parallel$GaAs[11$\bar{2}$] and the other with $I \parallel$GaAs[1$\bar{1}$0], is in fact theoretically anticipated because the intrinsic contribution in AHE is proportional to the integration of Berry curvature over the cuts of Fe(111) Fermi surface segment, thus it should have little dependence on the current direction on the same lattice plane. In both cases, the σ_{ah} vs σ_{xx}^2 plots for the thickest film (27 nm) show noticeable deviation from the fitting curve at the low temperature region. This deviation likely originates from the extrinsic mechanisms and will be discussed elsewhere.[32]

In Figs. 2(c), 3(a), and 3(b) a sign change of the AHE are observed clearly at low temperature for 27 nm film. Meanwhile, all the $-\sigma_{ah}$ vs σ_{xx}^2 plots in Figs. 3(a) and 3(b) show consistently negative slopes, in contrast to the fan-shape curves as in the case of Fe(001), where the slopes for thinner films are positive but turn negative for thicker films.[24] According to Eq. (1), the slope is determined by $\alpha\sigma_{xx0}^{-1} + \beta\sigma_{xx0}^{-2}$, which reflects the extrinsic mechanisms of the AHE. It is clearly suggested from the positive intercept b and negative slope that this sign change reflects the competition between the intrinsic AHE and the extrinsic mechanisms. To gain more insight we now try to derive the exact value of α and β. When $T \to 0$ K, the σ_{xx} in Eq. (1) is by definition equal to σ_{xx0}, therefore Eq. (1) is simplified into

$$-\sigma_{ah0} = \alpha\sigma_{xx0} + (\beta + b). \tag{2}$$

We fit the $-\sigma_{ah0}$ vs σ_{xx0} plot according to Eq. (2), and the result is presented in Fig. 4(a). We can therefore obtain the slope $\alpha = (-1.25 \pm 0.15) \times 10^{-2}$ and the intercept $(\beta + b) = (1126 \pm 106)\ \Omega^{-1}\ \mathrm{cm}^{-1}$, thus $\beta = 305\ \Omega^{-1}\ \mathrm{cm}^{-1}$. Notice that the value of α here is negative, about 3 times larger than the case of Fe(001)/GaAs(100).[24] This large skew scattering will dominate the total AHE at low temperature for thicker films, when the σ_{xx0} is large enough. So the negative anomalous Hall

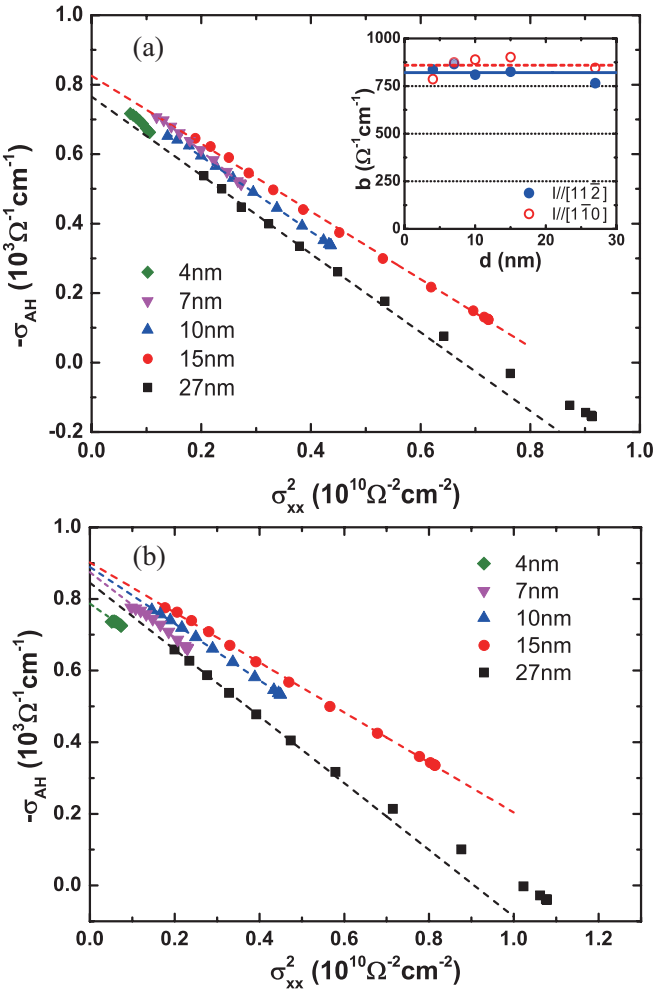

FIG. 3. (Color online) $-\sigma_{ah}$ vs σ_{xx}^2 for different thicknesses of Fe/GaAs(111) samples. The direction of the current is along (a) GaAs[11$\bar{2}$] and (b) GaAs[1$\bar{1}$0]. The dashed lines denote linear fitting following Eq. (1). The intercept b fitted from (a) and (b) are shown in the inset.

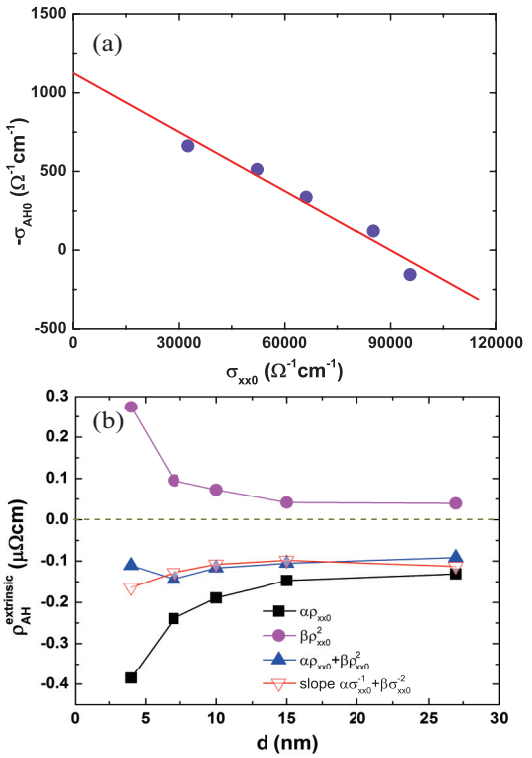

FIG. 4. (Color online) (a) The plot of $-\sigma_{ah0}$ vs σ_{xx0}. Here σ_{ah0} is the anomalous Hall conductivity at 5 K and σ_{xx0} is the longitudinal conductivity at 5 K. The red line represents linear fitting. (b) The extrinsic contributions to the anomalous Hall resistivity. The skew scattering contribution $\alpha\rho_{xx0}$ (black squares) and the side jump contribution $\beta\rho_{xx0}^2$ (purple dots), together with the sum $\alpha\rho_{xx0} + \beta\rho_{xx0}^2$ (solid blue triangles), are obtained via tuning the film thickness. The hollow red triangles represents the extrinsic anomalous Hall resistivity derived as the slopes of the fittings presented in Fig. 3(a).

resistivity in Fig. 2(c) should be attributed to the large skew scattering contribution.

To explicitly separate out the different contributions, combined Figs. 3(a) and 4(a), the extrinsic AHE can be studied independently by varying temperature and tuning thickness. We plot the thickness dependence of skew scattering $\alpha\rho_{xx0}$ and side jump $\beta\rho_{xx0}^2$ in Fig. 4(b), along with the sum $\alpha\rho_{xx0} + \beta\rho_{xx0}^2$ as the derived magnitude of extrinsic AHE. Meanwhile, as discussed previously, the extrinsic AHE can also be inferred from the slopes of the $-\sigma_{ah}$ vs σ_{xx}^2 plots in Fig. 3(a), in which σ_{xx} is tuned by varying temperature. The extrinsic mechanisms of the AHE derived from both experimental approaches are compared in Fig. 4(b), in which nice agreement is clearly shown.

In summary, we have investigated Fe(111)/GaAs(111) system and obtained the intrinsic AHC of Fe(111), the value is 821 Ω^{-1} cm^{-1}, which is smaller than the one of Fe(001) 1100 Ω^{-1} cm^{-1}. At the same time we clarified that the negative anomalous Hall resistivity found in our experiment is contributed by the skew scattering. These experimental results clearly show that the anisotropy of the intrinsic AHE exists in Fe single crystal. The value we report here is close to the value 842 Ω^{-1} cm^{-1} calculated by Weischenberg *et al.*,[13] although in their work the intrinsic AHC in Fe(111) was expected to be larger than that in Fe(001) (767 Ω^{-1} cm^{-1}). The discrepancy reflects the difficulty faced by *ab initio* calculations when tackling spin-orbital interaction related issues. We hope the experimental result presented here may intrigue more theoretical focuses on the anomalous Hall effect.

This work was supported by NSFC (No. 10834001), MOST (No. 2009CB929200, No. 2009CB929203), and MOE and SAFEA (No. B07020).

*Corresponding author: xfjin@fudan.edu.cn

[1] R. Karplus and J. M. Luttinger, Phys. Rev. **95**, 1154 (1954).
[2] J. M. Luttinger, Phys. Rev. **112**, 739 (1958).
[3] J. Smit, Physica **21**, 877 (1955).
[4] J. Smit, Physica **24**, 39 (1958).
[5] L. Berger, Phys. Rev. B **2**, 4559 (1970).

[6]G. Sundaram and Q. Niu, Phys. Rev. B **59**, 14915 (1999).
[7]T. Jungwirth, Q. Niu, and A. H. MacDonald, Phys. Rev. Lett. **88**, 207208 (2002).
[8]M. Onoda and N. Nagaosa, J. Phys. Soc. Jpn. **71**, 19 (2002).
[9]Z. Fang, N. Nagaosa, K. S. Takahashi, A. Asamitsu, R. Mathieu, T. Ogasawara, H. Yamada, M. Kawasaki, Y. Tokura, and K. Terakura, Science **302**, 92 (2003).
[10]Y. Yao, L. Kleinman, A. H. MacDonald, J. Sinova, T. Jungwirth, D.-s. Wang, E. Wang, and Q. Niu, Phys. Rev. Lett. **92**, 037204 (2004).
[11]D. Xiao, M.-C. Chang, and Q. Niu, Rev. Mod. Phys. **82**, 1959 (2010).
[12]E. Roman, Y. Mokrousov, and I. Souza, Phys. Rev. Lett. **103**, 097203 (2009).
[13]J. Weischenberg, F. Freimuth, J. Sinova, S. Blügel, and Y. Mokrousov, Phys. Rev. Lett. **107**, 106601 (2011).
[14]H. Zhang, S. Blügel, and Y. Mokrousov, Phys. Rev. B **84**, 024401 (2011).
[15]S. Kaya, Sci. Rep. Tohoku Univ. **17**, 1157 (1928).
[16]K. Honda and S. Kaya, Sci. Rep. Tohoku Univ. **15**, 721 (1926).
[17]N. V. Volkenshtein, G. V. Fedorov, and V. P. Shirokovskii, Phys. Met. Metallogr. **11**, 151 (1961).
[18]R. S. Lee and S. Legvold, Phys. Rev. **162**, 431 (1967).
[19]T. Hiraoka, J. Sci. Hiroshima Univ. Ser. A-2 **32**, 153 (1968).
[20]A. A. Hirsch and Y. Weissman, Phys. Lett. A **44**, 239 (1973).
[21]K. Ohgushi, S. Miyasaka, and Y. Tokura, J. Phys. Soc. Jpn. **75**, 013710 (2006).
[22]B. C. Sales, R. Jin, and D. Mandrus, Phys. Rev. B **77**, 024409 (2008).
[23]J. Stankiewicz and K. P. Skokov, Phys. Rev. B **78**, 214435 (2008).
[24]Y. Tian, L. Ye, and X. Jin, Phys. Rev. Lett. **103**, 087206 (2009).
[25]P. N. Dheer, Phys. Rev. **156**, 637 (1967).
[26]D. K. Biegelsen, R. D. Bringans, J. E. Northrup, and L.-E. Swartz, Phys. Rev. Lett. **65**, 452 (1990).
[27]O. K. Y. Endo, S. Okamoto, and Y. Shimada, J. Appl. Phys. **81**, 344 (1997).
[28]C. R. Tellier and A. J. Tosser, *Size Effects in Thin Films* (Elsevier, Amsterdam, 1982).
[29]D. Hou, Y. Li, D. Wei, D. Tian, L. Wu, and X. Jin, J. Phys.: Condens. Matter **24**, 482001 (2012).
[30]L. Ye, Y. Tian, X. Jin, and D. Xiao, Phys. Rev. B **85**, 220403 (2012).
[31]A. Shitade and N. Nagaosa, J. Phys. Soc. Jpn. **81**, 083704 (2012).
[32]D. Hou, Ph.D. thesis, Fudan University, 2012.